

Low-temperature sintering and microwave dielectric properties of $\text{Ba}_5\text{Nb}_4\text{O}_{15}$ – BaNb_2O_6 mixtures for LTCC applications

Dong-Wan Kim^a, Kug Sun Hong^{a,*}, Chong S. Yoon^b, Chang Kyung Kim^b

^a*School of Materials Science and Engineering, College of Engineering, Seoul National University, Shinrim-dong San 56-1, Kwanack-Ku, Seoul 151-742, South Korea*

^b*Department of Inorganic Materials Engineering, Division of Materials Science and Engineering, Hanyang University, Seoul, South Korea*

Abstract

The addition of B_2O_3 to $\text{Ba}_5\text{Nb}_4\text{O}_{15}$ – BaNb_2O_6 significantly lowered the sintering temperature to ~ 900 °C in comparison to ~ 1250 °C for samples without B_2O_3 . The presence of a B_2O_3 -rich intergranular phase in the sample was observed, which was attributed to the presence of a liquid phase during sintering. The barium metaniobate, BaNb_2O_6 has two polymorphs, with orthorhombic and hexagonal forms. A major contributor to microwave dielectric properties of low-fired samples is the low temperature phase, hexagonal BaNb_2O_6 . The small amount of hexagonal BaNb_2O_6 could tune τ_f of $\text{Ba}_5\text{Nb}_4\text{O}_{15}$. Therefore, $\text{Ba}_5\text{Nb}_4\text{O}_{15}$ – BaNb_2O_6 with B_2O_3 can be a suitable for low-temperature cofired ceramic (LTCC), due to its reduced sintering temperature and good microwave dielectric properties: $Q \times f = 28\,000$ GHz, ϵ_r and τ_f are 42 and 0 ppm/°C, respectively. The chemical compatibility of silver electrodes and low-fired samples has also been investigated.

© 2003 Elsevier Ltd. All rights reserved.

Keywords: Capacitors; Dielectric properties; Electron microscopy; Niobates; Sintering; BaNb_2O_6

1. Introduction

Low temperature cofired ceramic (LTCC) is finding increased usage as an interconnect substrate, especially in microwave applications due to the high conductivity of the conductors and low loss of the LTCC dielectrics. LTCC has the potential to incorporate multi-layer structures and buried passive components, with minimal processing steps, thus leading to very compact microwave subsystems.

The new family of LTCC materials can be addressed the growing demand of electronic manufacturers to reduce package size, minimize energy loss, and eliminate stray electromagnetic radiation. A survey of commercial LTCC materials shows that the vast majority of them have dielectric constants around 4–5 and 7–9 that provide high signal propagation speeds in a microcircuit. There are currently several types of LTCC materials in terms of chemistry. Many of materials are based on mixtures of low-melting glasses with alumina as a filler

for the dielectric tape. However, in certain applications low dielectric loss LTCC materials with higher dielectric constants in the range of 15–400 can offer design and functional benefits for electronic packaging without speed deterioration.^{1,2}

The dielectric and luminescence properties of $\text{Ba}_5\text{Nb}_4\text{O}_{15}$ have been investigated and it has been found to be a useful material in microwave communication applications.^{3,4} But, the literature has minimal information on the dielectric properties of BaNb_2O_6 . In this work, mixtures of $\text{Ba}_5\text{Nb}_4\text{O}_{15}$ and BaNb_2O_6 were prepared. Adjustment of the temperature coefficient of resonant frequency (τ_f) toward 0 ppm/°C can be achieved by modifying $\text{Ba}_5\text{Nb}_4\text{O}_{15}$ with BaNb_2O_6 of opposite τ_f . We also observed that a small addition of B_2O_3 to $\text{Ba}_5\text{Nb}_4\text{O}_{15}$ – BaNb_2O_6 mixtures significantly lowers the sintering temperature from 1250 °C without B_2O_3 additions to 900 °C. The focus of present study was to investigate the sintering mechanism and microwave dielectric properties of low-fired $\text{Ba}_5\text{Nb}_4\text{O}_{15}$ – BaNb_2O_6 mixtures. The compatibility with the electrodes is also addressed as a suitable candidate for LTCC applications.

* Corresponding author. Tel.: +822-880-8316; fax: +822-886-4156.
E-mail address: kshongss@plaza.snu.ac.kr (K. Sun Hong).

2. Experimental procedure

The starting raw materials used were high-purity (99.9%) BaCO_3 , and Nb_2O_5 . Mixtures of $\text{Ba}_5\text{Nb}_4\text{O}_{15}$ – BaNb_2O_6 powders of varying compositions were prepared using the conventional mixed oxide method and calcined at 1100 °C for 2 h. The calcined powders containing appropriate amount of B_2O_3 with 99.9% purity were ball-milled for 24 h using ethanol as a medium. The milled powders were then dried, granulated, and pressed at 1000 kg/cm² to form pellets with an 8 mm diameter and 3 mm thick. The pellets were sintered at 900–950 °C with a heating rate of 5 °C/min. Shrinkage of the specimens during heating was measured using a horizontal-loading dilatometer with alumina rams and boats (model DIL 402C, Netzsch Instruments, Germany).

The crystal structure of sintered samples was investigated using X-ray powder diffraction (model M18XHF, Macscience Instruments, Japan) in the 2θ range from 20 to 60°.

For cofiring experiments, the ceramic powder was mixed with 30 wt.% Ag and Cu powders, and cofired in air at 900 °C for 2 h, and in reducing atmosphere at 950 °C for 2 h, respectively. The oxygen partial pressure was adjusted by regulating the proportions of CO_2 and CO in mixtures to help prevent oxidation of Cu electrode.

Polished and thermally etched surfaces of sintered specimens were examined using field emission scanning electron microscopy (FESEM: model JSM-6330F, Jeol, Japan). Specimens for transmission electron microscopy (TEM: model JEM-3000F, Jeol, Japan) observation were mechanically thinned and Ar^+ -ion-beam milled after being mounted to 3-mm copper grids. The composition analysis was performed using energy-dispersive spectroscopy (EDS: model INCA, Oxford Instruments, Bucks, UK).

The microwave dielectric properties of sintered samples were measured at x -band frequencies (8–10 GHz) using a network analyzer (model HP8720C, Hewlett Packard, Palo Alto, CA).

3. Results and discussion

Fig. 1 shows the effect of a 0.3 wt.% B_2O_3 addition on the shrinkage behavior of $\text{Ba}_5\text{Nb}_4\text{O}_{15}$ – BaNb_2O_6 ceramics. The results demonstrate that the onset of shrinkage move towards much lower temperature with the addition of B_2O_3 . The shrinkage for samples with B_2O_3 appears to occur rapidly at ~ 850 °C and reaches a maximum value at ~ 950 °C. In contrast the shrinkage for undoped samples does not occur as rapidly. It is thought that B_2O_3 acts as a sintering aid for $\text{Ba}_5\text{Nb}_4\text{O}_{15}$ – BaNb_2O_6 mixtures.

The dense microstructure produced by the low firing of $\text{Ba}_5\text{Nb}_4\text{O}_{15}$ – BaNb_2O_6 was confirmed by a SEM

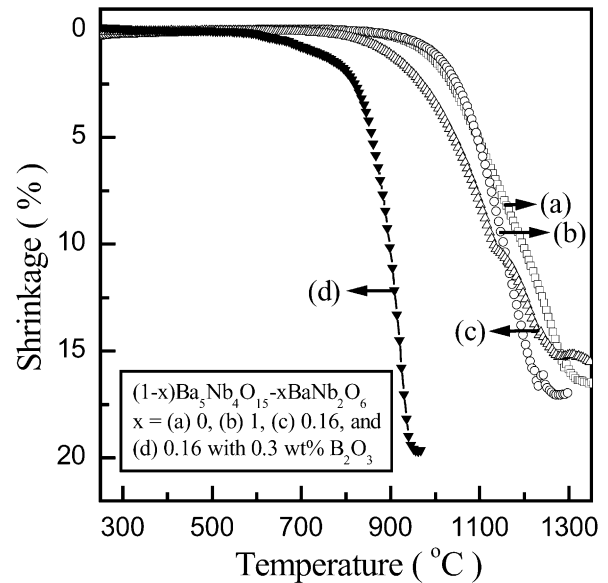


Fig. 1. Shrinkage of $(1-x)\text{Ba}_5\text{Nb}_4\text{O}_{15}-x\text{BaNb}_2\text{O}_6$ as a function of temperature: $x =$ (a) 0, (b) 1, (c) 0.16 without B_2O_3 , and (d) 0.16 with 0.3 wt.% B_2O_3 .

study. Fig. 2 shows typical SEM micrographs of $\text{Ba}_5\text{Nb}_4\text{O}_{15}$ – BaNb_2O_6 samples with 0.3 wt.% B_2O_3 sintered at 900 °C for 2 h. Sintered $\text{Ba}_5\text{Nb}_4\text{O}_{15}$ sample containing B_2O_3 had elongated grains with a small grain size range between 1 and 3 μm [Fig. 2(a)]. With the increase of BaNb_2O_6 content (x), the amount of faceted grains increased. We found the composition of the faceted grains to be BaNb_2O_6 using EDS analysis. The backscattered electron images demonstrate this result more clearly, as shown in Fig. 2(d). But, no second phase was observed. Generally, the liquid phase melts and is distributed along the grain boundaries during sintering where it solidifies into a second phase, in

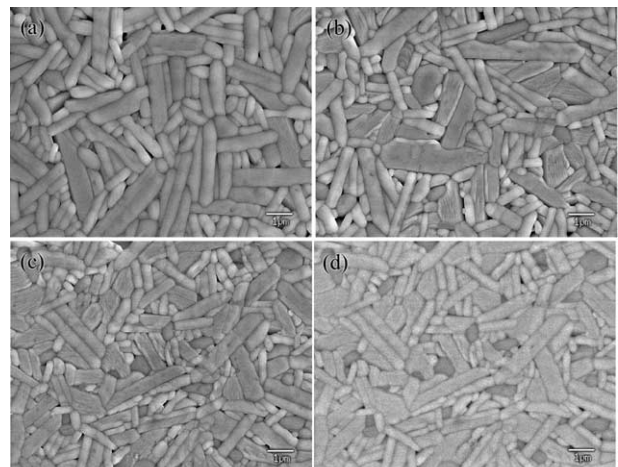


Fig. 2. Scanning electron micrographs of $(1-x)\text{Ba}_5\text{Nb}_4\text{O}_{15}-x\text{BaNb}_2\text{O}_6$ with 0.3 wt.% B_2O_3 samples sintered at 900 °C for 2 h: $x =$ (a) 0, (b) 0.1, (c) 0.16. (d) Backscattered electron image of (c) showing BaNb_2O_6 present.

low-fired samples.^{5,6} Close analysis is further required to examine the low-firing of B₂O₃-doped samples. Fig. 3 shows bright-field images and an EDS spectrum of a 0.84Ba₅Nb₄O₁₅–0.16BaNb₂O₆ sample with 0.3 wt.% B₂O₃ sintered at 900 °C for 2 h. In Fig. 3(a), the presence of an intergranular phase was observed. The inset

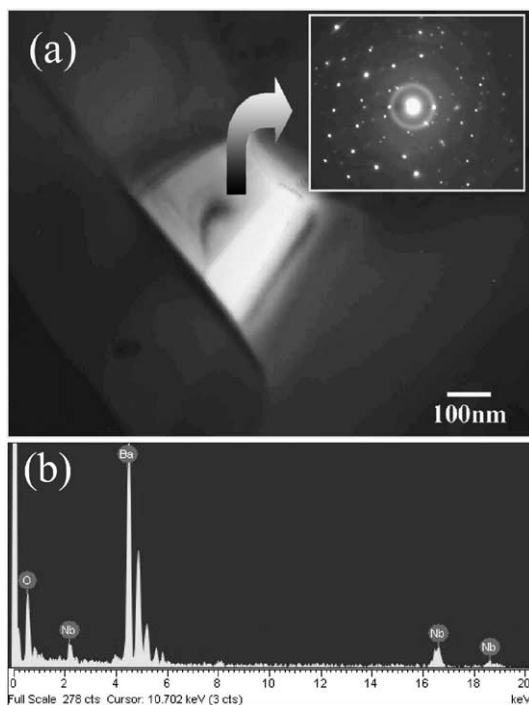


Fig. 3. (a) Bright-field image of 0.84Ba₅Nb₄O₁₅–0.16BaNb₂O₆ with 0.3 wt.% B₂O₃ sintered at 900 °C for 2 h. The inset shows SAD pattern of the intergranular phase. (b) EDS spectrum of the intergranular phase in (a).

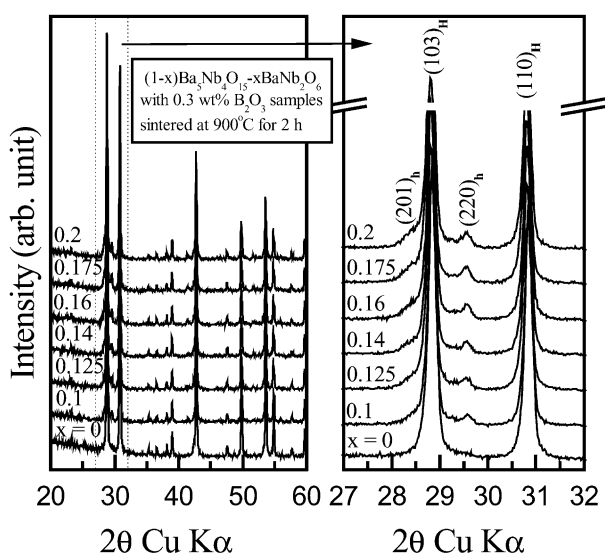


Fig. 4. XRD patterns of (1–*x*)Ba₅Nb₄O₁₅–*x*BaNb₂O₆ with 0.3 wt.% B₂O₃ samples sintered at 900 °C for 2 h showing the mixture phase (H: hexagonal Ba₅Nb₄O₁₅, h: hexagonal BaNb₂O₆).

shows a ring diffraction pattern of the intergranular phase which indicates that it is composed of microcrystals. From the EDS spectra of intergranular phases, the composition of the microcrystals was found to be a BaO-rich phase, as shown in Fig. 3(b).

In the phase diagram of BaO–B₂O₃, the BaB₈O₁₃–BaB₄O₇, BaB₄O₇–BaB₂O₄, BaB₂O₄–Ba₃B₂O₆ eutectics exist as low as 859, 889, 905 °C.⁷ Takada et al. suggested that eutectic liquid formation assisted in the densification of BaO–TiO₂–WO₃ with B₂O₃ additions.⁸ The low-firing of Ba₅Nb₄O₁₅–BaNb₂O₆ can be attributed to the formation of a B₂O₃-rich liquid phase containing BaO.

Fig. 4 shows the X-ray diffraction (XRD) profiles of the (1–*x*)Ba₅Nb₄O₁₅–*x*BaNb₂O₆ samples sintered at 900 °C for 2 h for compositions with varying BaNb₂O₆ mole fraction (*x*). In Fig. 4, it was confirmed that all samples were mixtures of Ba₅Nb₄O₁₅ and BaNb₂O₆ with no observable formation of a second phase. This is in agreement with a postulated phase equilibrium diagram reported previously by Roth and Waring.⁹ BaNb₂O₆ phase have been identified based on faceted morphology of these mixture regions, and relatively dark contrast to Ba₅Nb₄O₁₅, as shown in Fig. 2(d).

The BaNb₂O₆ has two polymorphic symmetries: orthorhombic and hexagonal.^{10,11} Closer analysis reveals that samples sintered at 900 °C for 2 h are mixtures of hexagonal Ba₅Nb₄O₁₅ and hexagonal BaNb₂O₆. According to XRD data of undoped mixture samples sintered at 1250 °C for 2 h, diffraction lines associated with BaNb₂O₆ were indexed as orthorhombic structure. The crystal structure of the orthorhombic sample transformed back into the hexagonal form when sintered at 900 °C for 2 h, contrary to other reports that the transformation is reversible.^{10,11}

Ba₅Nb₄O₁₅ had good microwave dielectric properties: $Q \times f = 57\,000$ GHz, $\epsilon_r = 41$, and τ_f of 50 ppm/°C. Hexagonal BaNb₂O₆ was difficult to sinter to high density because of hexagonal to orthorhombic transition at 1100 °C. For preparation of high density hexagonal BaNb₂O₆ samples, conventional hot uniaxial pressing was used, at temperature below 1100 °C. Hexagonal BaNb₂O₆ has a $Q \times f$ of 4000 GHz, ϵ_r of 42, and τ_f of –800 ppm/°C. From these results, hexagonal BaNb₂O₆ is a dominant factor of controlling microwave dielectric properties of low-fired Ba₅Nb₄O₁₅–BaNb₂O₆.

Fig. 5 shows the microwave dielectric properties of low-fired Ba₅Nb₄O₁₅–BaNb₂O₆ sintered at 900 °C for 2 h. The ϵ_r is nearly constant, due to the similar ϵ_r values of Ba₅Nb₄O₁₅ and hexagonal BaNb₂O₆. However, the small amount of hexagonal BaNb₂O₆ may contribute to approach a τ_f of 0 ppm/°C in low-fired samples because BaNb₂O₆ possesses a very large and negative τ_f value. It is noteworthy that the τ_f of low-fired 0.84Ba₅Nb₄O₁₅–0.16BaNb₂O₆ was modified to 0 ppm/°C. At this composition, a $Q \times f$ of 28000 GHz and ϵ_r of 42 were measured. A 0.16 mole fraction of BaNb₂O₆ is

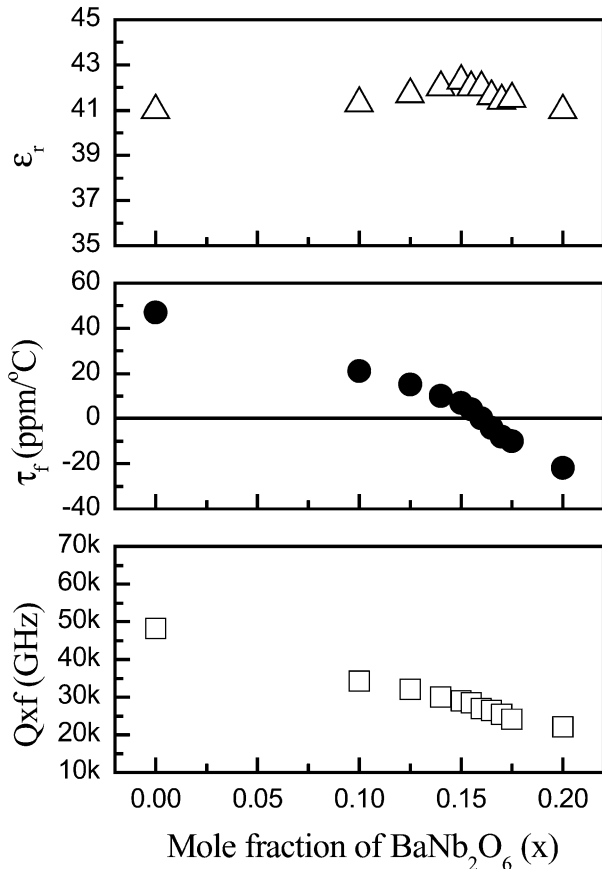


Fig. 5. Microwave dielectric properties of $(1-x)\text{Ba}_5\text{Nb}_4\text{O}_{15}-x\text{BaNb}_2\text{O}_6$ with 0.3 wt.% B_2O_3 samples sintered at 900°C for 2 h, as a function of mole fraction of BaNb_2O_6 (x).

equivalent of 0.063 volume fraction; therefore, the $Q \times f$ of $0.84\text{Ba}_5\text{Nb}_4\text{O}_{15}-0.16\text{BaNb}_2\text{O}_6$ is 31,000 GHz from a simple calculation based on the mixing rule of composites with two phases.¹² This value corresponds to the measured $Q \times f$, 28,000 GHz, as shown in Fig. 4. Generally, the addition of dopants to lower the sintering temperature is accompanied by a significant decrease in the microwave dielectric properties. But, the low-fired $\text{Ba}_5\text{Nb}_4\text{O}_{15}-\text{BaNb}_2\text{O}_6$ possesses excellent microwave dielectric properties because the small amount of liquid-forming compositions enabled low temperature sintering.

For compatibility tests, mixtures of ceramic powder with Ag and Cu powders were cofired and analyzed to detect interactions between the low-fired samples and electrodes. SEM analysis revealed no interaction forming new phases after firing, as shown in Fig. 6. This observation was also confirmed by no difference of the XRD profiles before and after firing. It is obvious that the reaction of low-fired $\text{Ba}_5\text{Nb}_4\text{O}_{15}-\text{BaNb}_2\text{O}_6$ with Ag and Cu electrodes did not occur. Therefore, $\text{Ba}_5\text{Nb}_4\text{O}_{15}-\text{BaNb}_2\text{O}_6$ with B_2O_3 could be selected as suitable candidates for LTCC materials, because of low

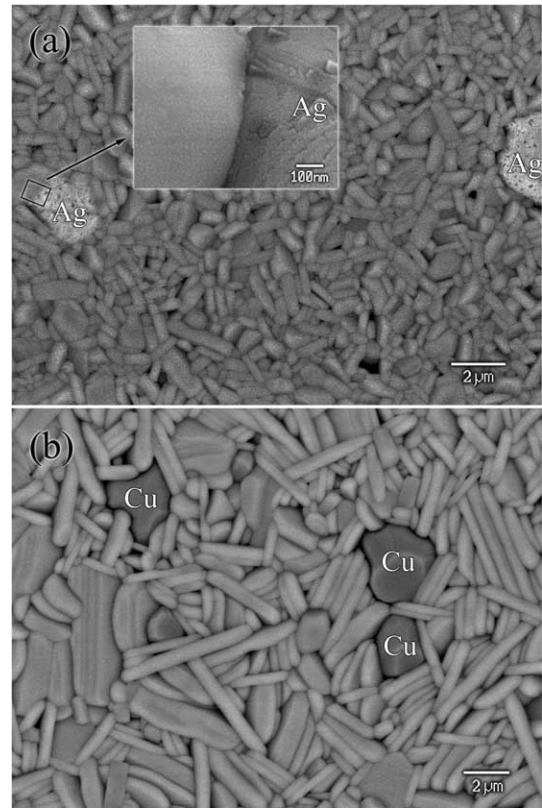


Fig. 6. Backscattered electron images of $0.84\text{Ba}_5\text{Nb}_4\text{O}_{15}-0.16\text{BaNb}_2\text{O}_6$ with 0.3 wt.% B_2O_3 samples (a) cofired with Ag powders in air at 900°C for 2 h and (b) cofired with Cu powders in 10^{-10} atm Po_2 at 950°C for 2 h.

sintering temperature, good microwave dielectric properties, and compatibility with electrodes.

A stripline resonator was built using standard multi-layer green tape processes for LTCC application. The stripline was designed to resonate at 1.9 GHz via a capacitive coupling to the input/output (I/O) pads. The low-fired $\text{Ba}_5\text{Nb}_4\text{O}_{15}-\text{BaNb}_2\text{O}_6$ has the lower dielectric loss ($\tan \delta$) than other LTCC materials with low dielectric constant. This is likely the reason that the low-fired $\text{Ba}_5\text{Nb}_4\text{O}_{15}-\text{BaNb}_2\text{O}_6$ have higher $Q \times f$.

4. Conclusion

$\text{Ba}_5\text{Nb}_4\text{O}_{15}-\text{BaNb}_2\text{O}_6$ with B_2O_3 low-fired at 900°C for 2 h can be mixtures of hexagonal $\text{Ba}_5\text{Nb}_4\text{O}_{15}$ and hexagonal BaNb_2O_6 . It was found that a small addition of B_2O_3 to $\text{Ba}_5\text{Nb}_4\text{O}_{15}-\text{BaNb}_2\text{O}_6$ enabled a reduction in sintering temperature to 900°C , from 1250°C due to the formation of $\text{BaO}-\text{B}_2\text{O}_3$ liquid phases. The low-fired $\text{Ba}_5\text{Nb}_4\text{O}_{15}-\text{BaNb}_2\text{O}_6$ possesses excellent microwave dielectric properties due to the small amount of liquid-forming compositions. The τ_f of $\text{Ba}_5\text{Nb}_4\text{O}_{15}$ can be continuously adjusted, including 0 ppm/ $^\circ\text{C}$, depending on the amount of BaNb_2O_6 with a large and negative τ_f . At a composition of $0.84\text{Ba}_5\text{Nb}_4\text{O}_{15}-0.16\text{BaNb}_2\text{O}_6$ with

0.3 wt.% B_2O_3 , $Q \times f$ is 28,000 GHz, ϵ_r and τ_f are 42 and 0 ppm/°C, respectively. Also, this material is compatible with Ag and Cu electrodes, therefore, is suitable for LTCC applications.

References

1. Jones, W. K., Liu, Y., Larsen, B., Wang, P. and Zampino, M. Chemical, structural and mechanical properties of the LTCC tapes. In *Proceedings of the 2000 International Symposium on Microelectronics*. IMAPS, Boston, MA, USA, 2000, pp. 669–704.
2. Kniajer, G., Dechant, K. and Apté, P. Low loss, low temperature cofired ceramics with higher dielectric constants for multichip modules (MCM). In *Proceedings of the 1997 International Conference on Multichip Modules*. IEEE, Piscataway, NJ, USA, 1997, pp. 121–127.
3. Srivastava, A. M. and Ackerman, J. F., On the luminescence of $Ba_5M_4O_{15}$ ($M = Ta^{5+}, Nb^{5+}$). *J. Solid State Chem.*, 1997, **134**, 187–191.
4. Ratheesh, R., Sebastian, M. T., Mohanan, P., Tobar, M. E., Hartnett, J., Woode, R. and Blair, D. G., Microwave characterization of $BaCe_2Ti_5O_{15}$ and $Ba_5Nb_4O_{15}$ ceramics dielectric resonators using whispering gallery mode method. *Mater. Lett.*, 2000, **45**, 279–285.
5. Kim, D. W., Ko, K. H. and Hong, K. S., Influence of copper(II) oxide additions to zinc niobate microwave ceramics on sintering temperature and dielectric properties. *J. Am. Ceram. Soc.*, 2001, **84**, 1286–1290.
6. Kim, D. W., Hong, H. B. and Hong, K. S., Structural transition and microwave dielectric properties of $ZnNb_2O_6$ - TiO_2 sintered at low temperatures. *Jpn. J. Appl. Phys.*, 2002, **41**, 1465–1469.
7. Levin, E. M. and McMurdie, H. F., The system BaO - B_2O_3 . *J. Res. Natl. Bur. Stand.*, 1949, **42**, 131–138.
8. Takada, T., Wang, S. F., Yoshikawa, S., Jang, S. J. and Newnham, R. E., Effect of glass additions on BaO - TiO_2 - WO_3 microwave ceramics. *J. Am. Ceram. Soc.*, 1994, **77**, 1909–1916.
9. Roth, R. S. and Waring, J. L., Phase equilibrium relations in the binary system barium oxide–niobium pentoxide. *J. Res. Natl. Bur. Stand.*, 1961, **65**, 337–344.
10. Kovba, L. M., Lykova, L. N., Kulikova, Z. Y., Leshchenko, P. P. and Zapasskaya, I. P., Polymorphism of barium niobate $BaNb_2O_6$. *Moscow Univ. Chem. Bull.*, 1978, **33**, 69–71.
11. Yamaguchi, O., Matsui, K. and Shimizu, K., Crystallization of hexagonal $BaNb_2O_6$. *J. Am. Ceram. Soc.*, 1985, **68**, 173–175.
12. Kim, D. W., Park, B., Chung, J. H. and Hong, K. S., Mixture behavior and microwave dielectric properties in the low-fired TiO_2 - CuO system. *Jpn. J. Appl. Phys.*, 2000, **39**, 2696–2700.